

Disclosing phonon squeezing by non-equilibrium optical experiments

Martina Esposito^{1,†}, Kelvin Titimbo^{1,2,†}, Klaus Zimmermann^{1,2}, Francesca Giusti¹, Francesco Randi¹, Davide Boschetto³, Fulvio Parmigiani^{1,4}, Roberto Floreanini², Fabio Benatti^{1,2,*} and Daniele Fausti^{1,4,*}

¹Dipartimento di Fisica, Università di Trieste, 34127 Trieste, Italy

²Istituto Nazionale di Fisica Nucleare, Sezione di Trieste, 34014 Trieste, Italy

³Laboratoire d'Optique Appliquée, ENSTA ParisTech, CNRS, Ecole polytechnique, Université Paris-Saclay, 828 bd des Maréchaux, 91762 Palaiseau cedex, France

⁴Sincrotrone Trieste S.C.p.A., 34127 Basovizza, Italy

† These authors contributed equally to the work

* Corresponding authors.

May 5, 2022

Fluctuations of the atomic positions are at the core of a large class of unusual material properties ranging from quantum para-electricity and charge density wave to, possibly, high temperature superconductivity [1–7]. Their measurement in solids is subject of an intense scientific debate [8–14] focused on the research of a methodology capable of establishing a direct link between the variance of the ionic displacements and experimentally measurable observables. Here we address this issue by means of non-equilibrium optical experiments performed in shot-noise limited regime. The variance of the time dependent atomic positions and momenta is directly mapped into the quantum fluctuations of the photon number of the scattered probing light. A fully quantum description of the non-linear interactions between photonic and phononic fields unveils evidences of squeezing of thermal phonons in α -quartz.

The most common approach to squeezed vibrational states is based on non-equilibrium optical spectroscopy, where an ultrafast optical pulse (pump) impulsively perturbs the lattice and a properly time-delayed ultrafast probe pulse measures the time evolution of the ionic displacements revealing an oscillating response at frequencies characteristic of the excited vibrational modes [15–24]. In the non-linear spectroscopy formalism, the excitation mechanism of phonon states in transparent materials is called impulsive stimulated Raman scattering (ISRS) [21, 25]. The third order susceptibility tensor $\chi^{(3)}$ connects the induced polarization $P^{(3)}$ to three fields: $\mathcal{E}_1(\omega_1)$, probe field and $\mathcal{E}_2(\omega_2)$ and $\mathcal{E}_3(\omega_3)$, pump fields. In conventional two pulses pump and probe experiments, the fields $\mathcal{E}_2(\omega_2)$ and $\mathcal{E}_3(\omega_3)$ are two different frequency components of the pump laser pulse. In particular, all photon pairs $\omega_3 - \omega_2 = \Omega$, matching the frequency Ω of the stimulated Raman active vibrational mode, give ISRS [26]. The interaction of the probe field $\mathcal{E}_1(\omega_1)$ with the photo-excited material induces an emitted field, $\mathcal{E}_{EF}(\omega)$ which carries the information about the specific Raman mode excited in the crystal.

We choose a polarization configuration such to excite E -symmetry Raman optical modes in α -quartz and get an emitted field with polarization orthogonal to the probe one [27] (see supplementary information). We use a single pulse differential acquisition system in the shot-noise regime which provides a direct way to reconstruct the photon number quantum statistics of the scattered probe pulses. For a given time delay τ a reference pulse, which has not interacted with the sample, is subtracted from each pulse transmitted through the sample by a differential detector capable of single pulse acquisition. The integral of the voltage produced by the i -th differential pulse constitutes the measurement of the transmittance variation $\Delta T_i(\tau)$. The differential acquisition is repeated for $N = 8000$ pulses so that the mean value $\Delta T_{mean}(\tau) = \frac{1}{N} \sum_i \Delta T_i(\tau)$ and the variance $\Delta T_{var}(\tau) = \frac{1}{N} \sum_i [\Delta T_i(\tau) - \Delta T_{mean}(\tau)]^2$ is computed for each time delay τ . The experiment is performed in noise conditions limited by photon-number quantum fluctuations. The shot-noise characterization of the detection apparatus is reported in supplementary information.

The time domain response is shown in Fig 1 (a) for a representative pump fluence of 14 mJ/cm^2 . The blue curve depicts the time evolution of the transmittance mean value ΔT_{mean} and the red curve the time-evolution of its variance ΔT_{var} for the same data set. The Fourier transform of the mean has a single peak which is ascribed to the E -symmetry quartz vibrational mode with frequency $\Omega = 128 \text{ cm}^{-1} = 3.84 \text{ THz}$ [28]. The same frequency component is observed in the variance. In addition, a second peak at twice the phonon frequency appears exclusively in the variance. This feature is strongly suggestive of phonon squeezing [10]. A wavelet analysis of the variance oscillations allows a better study of the two frequency components (Fig 1 (b)): one notices that, while the fundamental frequency survives for tens of picoseconds, the 2Ω component vanishes within the first

two picoseconds.

In order to address the fingerprint of the squeezed nature of the photo-excited vibrational state, we provide here a fully quantum model for time domain experiments. Standard theoretical descriptions of ISRS adopt semi classical approaches where the dipolar interactions in the crystal are treated quantum mechanically while the optical fields are described classically [25]. In order to describe the measured photon-number quantum fluctuations of the probe field, we developed a novel approach which goes beyond semi-classical models and treats quantum mechanically both the material and the optical fields involved in the non-linear processes [29]. In this frame the first step is to adopt a quantized description for the mode-locked pulsed laser fields [30]. Each mode of frequency $\omega_j = \omega_0 + j\delta$, where ω_0 is the pulse central frequency, δ is a constant depending on the laser repetition rate and j is an integer, is quantized and described by single mode creation and annihilation operators \hat{a}_j^\dagger and \hat{a}_j . In this framework ISRS can be described by means of an effective interaction Hamiltonian which is descriptive of both the pumping and the probing processes. In both the processes two optical fields with orthogonal polarizations (denoted with subscript x or y) are involved: two pump fields in the pumping process and the probe and the emitted field in the probing process. The interaction Hamiltonian has the form

$$\mathcal{H} = \sum_{j,j'=-M}^M [g_{j,j'}^1 \mu_d (\hat{a}_{xj}^\dagger \hat{a}_{yj'} \hat{b}^\dagger + \hat{a}_{xj} \hat{a}_{yj'}^\dagger \hat{b}) + g_{j,j'}^2 \mu_s (\hat{a}_{xj}^\dagger \hat{a}_{yj'} (\hat{b}^\dagger)^2 + \hat{a}_{xj} \hat{a}_{yj'}^\dagger \hat{b}^2)], \quad (1)$$

where \hat{b} and \hat{b}^\dagger are the phonon annihilation and creation operators, μ_d and μ_s are complex coupling constants and the functions $g_{j,j'}^\ell$ take into account the relations between the frequencies of the involved fields,

$$g_{j,j'}^\ell = \begin{cases} 1 & \text{if } j' = j + \frac{\ell\Omega}{\delta} \\ 0 & \text{elsewhere,} \end{cases} \quad \ell = 1, 2,$$

with Ω the phonon frequency. A complete interaction Hamiltonian should contain also second order processes involving phonons with opposite momenta. However, since the probe detects only the $K = 0$ optical transition, we can make use of an effective Hamiltonian that accounts only for second order process involving this kind of phonons. The whole theoretical description of the experiment can be rationalized in a four step process as sketched in Fig 2: generation of phonon states in the pumping process (i), evolution of the produced vibrational state (ii), probing process (iii) and read out of the emitted photon observables (iv).

(i) Initially, the sample is in thermal equilibrium and it is described by a thermal phonon state ρ_β , at inverse temperature β . The laser pump pulse is described by a multimode coherent state of high intensity $|\bar{\nu}\rangle = |\nu_{-M}\rangle \otimes \dots \otimes |\nu_M\rangle$, where $|\nu_j\rangle$ are single mode coherent states associated with all the frequency components within the pulse. Each $|\nu_j\rangle$ is an eigenstate of the annihilation operator \hat{a}_j of photons in the mode of frequency ω_j , $\hat{a}_j |\nu_j\rangle = \nu_j |\nu_j\rangle$. We indicate with $\bar{\nu}$ the vector whose components are the amplitudes ν_j . The equilibrium (pre-pump) photon-phonon state $\rho = |\bar{\nu}\rangle \langle \bar{\nu}| \otimes \rho_\beta$ is instantaneously transformed into $\rho^{\bar{\nu}} = \mathcal{U} \rho \mathcal{U}^\dagger$ by means of the unitary operator $\mathcal{U} = \exp\{-i\mathcal{H}\}$. Since the pumping operator \mathcal{U} acts on a high intensity photon coherent state $\bar{\nu}$, we can use the mean field approximation for the photon degrees of freedom and replace \hat{a} with ν and \hat{a}^\dagger with ν^* for both the pump modes involved in (1), thus replacing \mathcal{U} by

$$\mathcal{U}_{\bar{\nu}} = \exp\{-i \sum_{j,j'=-M}^M [g_{j,j'}^1 \mu_d (\nu_{xj}^* \nu_{yj'} \hat{b}^\dagger + \nu_{xj} \nu_{yj'}^* \hat{b}) + g_{j,j'}^2 \mu_s (\nu_{xj}^* \nu_{yj'} (\hat{b}^\dagger)^2 + \nu_{xj} \nu_{yj'}^* \hat{b}^2)]\}. \quad (2)$$

The evolution operator generates coherent and squeezed phonon states, respectively, through the linear and quadratic terms in the phonon operators \hat{b} and \hat{b}^\dagger . The initial state $\rho^{\bar{\nu}}$ contains information about both photons and phonons. Tracing over the photon degrees of freedom, the resulting state $\rho_{II}^{\bar{\nu}}$ describes the excited phonons brought out of equilibrium by the impulsive pump process.

(ii) The time evolution of the excited phonons is described by using an open quantum systems approach, namely by means of a suitable master equation of Lindblad form that takes into account, besides the quantum unitary evolution, also the dissipative and noisy effects due to the interaction with a thermal environment.

(iii) The incoming probe pulses are in the multimode coherent state $|\bar{\alpha}\rangle$. The probing process at time τ is described by the same impulsive unitary operator \mathcal{U} used for the pump. However, in this case we can apply the mean field approximation only to the probe photon operators with x polarization, which correspond to a much more intense field than those with y polarization. Moreover, since the probe field is much weaker than the pump field, the quadratic terms in the interaction Hamiltonian in (1) can now be neglected. The unitary operator is

$$\mathcal{U}_{\bar{\alpha}'} = \exp\{-i\|\bar{\alpha}'\|(\hat{A}(\bar{\alpha}') \hat{b}^\dagger + \hat{A}^\dagger(\bar{\alpha}') \hat{b})\}, \quad \hat{A}(\bar{\alpha}') = \frac{1}{\|\bar{\alpha}'\|} \sum_{j=-M}^M (\alpha'_j)^* \hat{a}_{yj}, \quad (3)$$

where $\bar{\alpha}'$ is the vector with components $\alpha'_j = \mu_d \sum_{j'=-M}^M g_{j',j}^1 \alpha_{xj'}$ and $\hat{A}(\bar{\alpha}')$ is a collective photon annihilation operator such that $[\hat{A}(\bar{\alpha}'), \hat{A}^\dagger(\bar{\alpha}')]=1$.

The latter unitary operator acts on a state of the form $|\bar{\alpha}\rangle\langle\bar{\alpha}| \otimes \rho_{II}^{\bar{\nu}}(\tau)$. The information about the phonons are extracted by measuring the emitted field photons. In particular, the emitted photon state $\rho_I(\tau)$ is obtained by tracing away the phonon degrees of freedom.

(iv) The possible quantum features of the phonon state, e.g. squeezing, can be read off as they are imprinted into $\rho_I(\tau)$. In particular for each time delay τ we can compute the quantities $\langle\hat{N}_y\rangle = \hat{A}^\dagger(\bar{\alpha}')\hat{A}(\bar{\alpha}')$ and $\Delta^2 \hat{N}_y = \langle\hat{N}_y^2\rangle - \langle\hat{N}_y\rangle^2$, which are exactly the observables measured in the experiment, that is the mean value and the variance of the number of photons of the emitted field. The details of the theoretical model are reported in supplementary information. The theoretical results for $\mu_s = 0$ and $\mu_s \neq 0$ are shown in Fig 3 together with the corresponding wavelet analysis for the variance of the number of emitted photons. The calculations reproduce the experimental results in Fig 1, revealing a 2Ω frequency component in the variance, only when the pump creates squeezed phonon states ($\mu_s \neq 0$).

The proposed effective interaction model is further validated by a pump fluence dependence study. Fig 4 shows the amplitude $A_{2\Omega}$ of the 2Ω peak in the Fourier transform of the variance as a function of the pump fluence. The model predictions (continuous line) agree with the experimental data only in presence of a pump-induced squeezing of the phonon mode. The increase of $A_{2\Omega}$ with pump fluence allows us to give a direct estimation of the uncertainties of the phonon conjugated quadratures which are reported in the inset of Fig 4 for the different excitation fluencies (calculation details are given in supplementary information). The fluctuations of the time dependent atomic positions and momenta are mapped directly into the quantum fluctuations of the probe photon number, thereby providing an absolute reference for the vibrational quantum noise.

Finally, the generality of our fully quantum approach, used here to reveal the squeezed nature of photo-excited phonon states in quartz, offers a novel framework to unveil distinctive quantum properties of vibrational states in matter. This paves the way for future studies addressing the thermodynamics of lattice and molecular vibrations of complex systems, possibly, in quantum regimes.

Acknowledgments

The authors are grateful to John Goold, Roberto Merlin, Keith Nelson, Mauro Paternostro and Charles Shank for the insightful discussions and critical reading of the manuscript. We thank the *CAEN* company for the project and the realization of the differential detector used in the experiments. We acknowledge Giovanni Franchi for the design of the detector and Riccardo Tommasini for support during its development. The experimental activities have been carried out at the TRex labs within the Fermi project at Trieste's synchrotron facility. This work has been supported by a grant from the University of Trieste ('FRA 2013').

Author contributions

M.E., F.G., F.R., D.B. and D.F. performed the experiments. K.T., K.Z., R.F. and F.B. developed the theoretical description. M.E., F.G. and D.F. analyzed the experimental data, M.E., D.F., F.B. and F.P. coordinated the project and wrote the manuscript with contributions from all the co-authors. The experiment has been conceived by D.F and F.P.

Competing financial interests

The authors declare no competing financial interests.

References

- [1] Subir Sachdev. Quantum criticality: Competing ground states in low dimensions. *Science*, 288(5465):475–480, 2000.
- [2] Shunsuke Nozawa, Toshiaki Iwazumi, and Hitoshi Osawa. Direct observation of the quantum fluctuation controlled by ultraviolet irradiation in SrTiO_3 . *Phys. Rev. B*, 72:121101, 2005.
- [3] D. M. Newns and C. C. Tsuei. Fluctuating cu-o-cu bond model of high-temperature superconductivity. *Nature Physics*, 184(191):1745–2473, 2007.
- [4] K. Hashimoto, K. Cho, T. Shibauchi, S. Kasahara, Y. Mizukami, R. Katsumata, Y. Tsuruhara, T. Terashima, H. Ikeda, M. A. Tanatar, H. Kitano, N. Salovich, R. W. Giannetta, P. Walmsley, A. Carrington, R. Prozorov, and Y. Matsuda. A sharp peak of the zero-temperature penetration depth at optimal composition in $\text{baf}e2(\text{as}1\text{x}96\text{px})2$. *Science*, 336(6088):1554–1557, 2012.

[5] C. Castellani, C. Di Castro, and M. Grilli. Non-fermi-liquid behavior and d-wave superconductivity near the charge-density-wave quantum critical point. *Zeitschrift für Physik B Condensed Matter*, 103(2):137–144, 1996.

[6] K Alex Müller, W Berlinger, and E Tosatti. Indication for a novel phase in the quantum paraelectric regime of srtio3. *Zeitschrift für Physik B Condensed Matter*, 84(2):277–283, 1991.

[7] J. D. Cohen, S. M. Meenehan, G. S. MacCabe, S. Groblacher, A. H. Safavi-Naeini, F. Marsili, M. D. Shaw and O. Painter. Phonon counting and intensity interferometry of a nanomechanical resonator. *Nature*, 520:522–525, 2015.

[8] G. Garrett, A. Rojo, A. Sood, J. Whitaker, and R. Merlin. Vacuum Squeezing of Solids: Macroscopic Quantum States Driven by Light Pulses. *Science*, 275(5306):1638–1640, 1997.

[9] Gregory Garrett, John Whitaker, Ajay Sood, and Roberto Merlin. Ultrafast optical excitation of a combined coherent-squeezed phonon field in srtio3. *Opt. Express*, 1(12):385–389, 1997.

[10] O. V. Misochko, K. Sakai, and S. Nakashima. Phase-dependent noise in femtosecond pump-probe experiments on bi and gaas. *Phys. Rev. B*, 61:11225–11228, 2000.

[11] Xuedong Hu and Franco Nori. Phonon squeezed states: quantum noise reduction in solids. *Physica B: Condensed Matter*, 263-264:16–29, 1999.

[12] Xuedong Hu and Franco Nori. Quantum phonon optics: Coherent and squeezed atomic displacements. *Phys. Rev. B*, 53:2419–2424, 1996.

[13] Bartels, Albrecht and Dekorsy, Thomas and Kurz, Heinrich. Impulsive Excitation of Phonon-Pair Combination States by Second-Order Raman Scattering. *Phys. Rev. Lett.*, 84:2981–2984, 2000.

[14] A. Hussain and S. R. Andrews. Absence of phase-dependent noise in time-domain reflectivity studies of impulsively excited phonons. *Phys. Rev. B*, 81:224304, 2010.

[15] Dhar, Rogers, and Nelson. Time-resolved vibrational spectroscopy in the impulsive limit. *Chem. Rev.*, 94:157, 1994.

[16] Johnson, S. L. and Beaud, P. and Vorobeva, E. and Milne, C. J. and Murray, É. D. and Fahy, S. and Ingold, G. Directly Observing Squeezed Phonon States with Femtosecond X-Ray Diffraction. *Phys. Rev. Lett.*, 102:175503, 2009.

[17] Trigo, M. et al. Fourier-transform inelastic X-ray scattering from time- and momentum-dependent phonon-phonon correlations. *Nat Phys*, 9:790–794, (2013).

[18] Ultrafast bond softening in bismuth: Mapping a solid’s interatomic potential with x-rays. *Solid State Commun.*, 102:207–220, 1997.

[19] E. Papalazarou, J. Faure, J. Mauchain, M. Marsi, A. Taleb-Ibrahimi, I. Reshetnyak, A. van Roekeghem, I. Timrov, N. Vast, B. Arnaud, and L. Perfetti. Coherent phonon coupling to individual bloch states in photoexcited bismuth. *Phys. Rev. Lett.*, 108:256808, 2012.

[20] J. J. Li, J. Chen, D. A. Reis, S. Fahy, and R. Merlin. Optical probing of ultrafast electronic decay in bi and sb with slow phonons. *Phys. Rev. Lett.*, 110:047401, 2013.

[21] Andrew M Weiner, Gary P Wiederrecht, Keith A Nelson, and DE Leaird. Femtosecond multiple-pulse impulsive stimulated raman scattering spectroscopy. *JOSA B*, 8(6):1264–1275, 1991.

[22] H. J. Zeiger, J. Vidal, T. K. Cheng, E. P. Ippen, G. Dresselhaus, and M. S. Dresselhaus. Theory for displacive excitation of coherent phonons. *Phys. Rev. B*, 45:768–778, 1992.

[23] Ahmed I. Lobad and Antoinette J. Taylor. Coherent phonon generation mechanism in solids. *Phys. Rev. B*, 64:180301, 2001.

[24] Xuedong Hu and Franco Nori. Phonon squeezed states generated by second-order raman scattering. *Phys. Rev. Lett.*, 79:4605–4608, 1997.

[25] Shaul Mukamel. *Principles of Nonlinear optical spectroscopy*. Oxford University Press, 1995.

[26] Stevens, T. E. and Kuhl, J. and Merlin, R. Coherent phonon generation and the two stimulated Raman tensors. *Phys. Rev. B*, 65:144304, 2002.

- [27] Andy Rundquist, Jon Broman, David Underwood, and David Blank. Polarization-dependent detection of impulsive stimulated raman scattering in alpha-quartz. *Journal of Modern Optics*, 52, 2006.
- [28] Scott and Porto. Longitudinal and transverse optical lattice vibrations in quartz. *Physical Review*, 161, 1967.
- [29] Kelvin Titimbo. *Creation and detection of squeezed phonons in pump and probe experiments: a fully quantum treatment*. PhD thesis, University of Trieste, 2015.
- [30] M Esposito, F Benatti, R Floreanini, S Olivares, F Randi, K Titimbo, M Pividori, F Novelli, F Cilento, F Parmigiani, and D Fausti. Pulsed homodyne gaussian quantum tomography with low detection efficiency. *New Journal of Physics*, 16(4):043004, 2014.

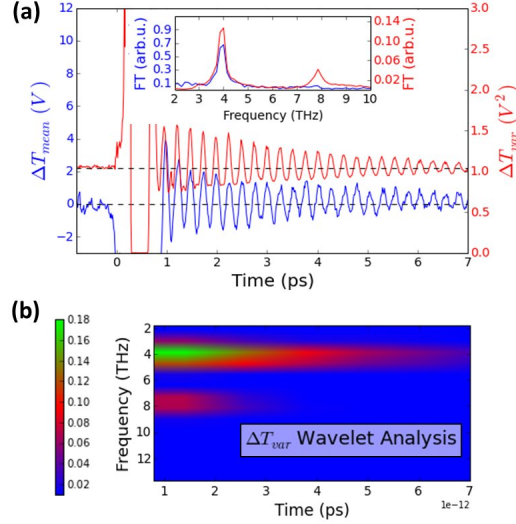


Figure 1: Pump probe experimental results for 14 mJ/cm^2 pump fluence. (a) Time resolved mean and variance of the transmittance variation. In the inset the Fourier transforms of the oscillating parts are reported. (b) Wavelet analysis of the variance oscillating part.

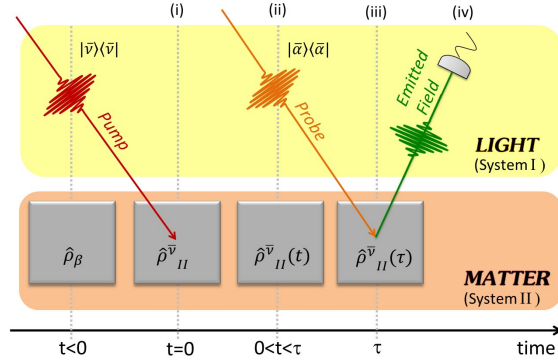


Figure 2: Sketch of the proposed four step effective model. The photon and phonon system are denoted with I and II, respectively.

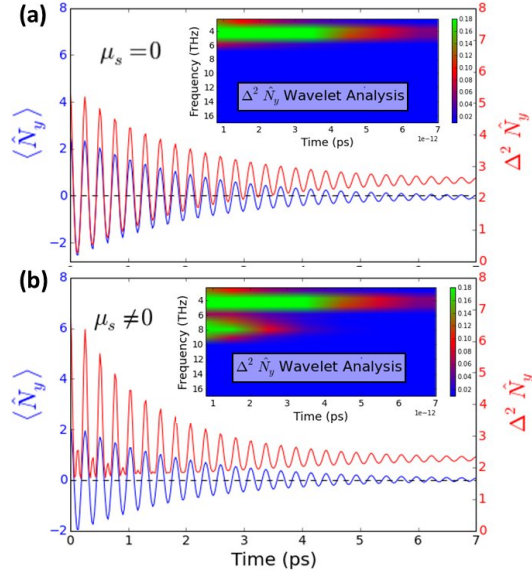


Figure 3: Theoretical calculations of the mean value and the variance of the number of photons of the emitted field. Comparison between the case with squeezing coupling constant $\mu_s = 0$ (a) and $\mu_s \neq 0$ (b). A wavelet analysis of the variance is reported in the insets for both cases.

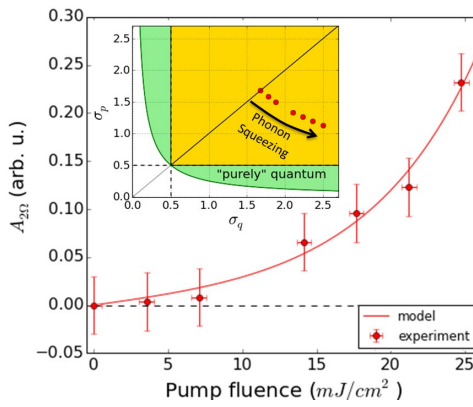


Figure 4: Amplitude $A_{2\Omega}$ of the 2Ω peak of the Fourier Transform of the variance. Comparison between experiments and theory as a function of the pump fluence. In the inset the uncertainties for the phonon position and momentum operators calculated from the model are plotted for the corresponding pump fluences.

Supplementary Information

Disclosing phonon squeezing by non-equilibrium optical experiments

Martina Esposito^{1,†}, Kelvin Titimbo^{1,2,†}, Klaus Zimmermann^{1,2}, Francesca Giusti¹, Francesco Randi¹,
Davide Boschetto³, Fulvio Parmigiani^{1,4}, Roberto Floreanini², Fabio Benatti^{1,2,*} and Daniele Fausti^{1,4,*}

¹Dipartimento di Fisica, Università di Trieste, 34127 Trieste, Italy

²Istituto Nazionale di Fisica Nucleare, Sezione di Trieste, 34014 Trieste, Italy

³Laboratoire d'Optique Appliquée, ENSTA ParisTech, CNRS, Ecole polytechnique,
Université Paris-Saclay, 828 bd des Maréchaux, 91762 Palaiseau cedex, France

⁴Sincrotrone Trieste S.C.p.A., 34127 Basovizza, Italy

† These authors contributed equally to the work

* Corresponding authors.

May 5, 2022

Polarization dependent ISRS in quartz

Impulsive stimulated Raman scattering (ISRS) is a non resonant excitation mechanism of lattice vibrations in transparent materials by ultrashort laser pulses. It is a four-wave mixing process due to third order polarization effects. The Cartesian components of the third order non-linear polarization are given by

$$P_i^{(3)}(\omega) = \sum_{jkl} \chi_{ijkl}^{(3)} [\mathcal{E}_1(\omega_1)]_j [\mathcal{E}_2(\omega_2)]_k [\mathcal{E}_3(\omega_3)]_l, \quad (1)$$

where $\chi_{ijkl}^{(3)}$ is the susceptibility tensor, \mathcal{E}_1 is the probe field and \mathcal{E}_2 and \mathcal{E}_3 are the pump fields. The susceptibility tensor determines the polarization selection of vibrational modes that can be excited via ISRS [1].

In particular, quartz Raman active vibrational modes are 4 totally symmetric modes of symmetry A_1 and 8 doubly degenerate modes of symmetry E (transverse and longitudinal) [2].

In our experiment, the sample is a 1 mm thick α -quartz, oriented in order to have the principal symmetry axis parallel to the probe propagation direction. A scheme of the chosen experimental geometry is shown in Fig 1. Both pump and probe come from the same laser source, a 250 kHz mode-locked amplified Ti:Sapphire system. The excited phonon state is detected via the scattering of the probe pulse which arrives on the sample with time delay τ with respect to the pump. The transmitted light undergoes a polarization selection through a polarizer positioned after the sample.

The pump direction is almost collinear with the probe one. Assuming that the involved optical fields propagate along the z direction, we can limit our analysis to the xy plane. In this case the quartz Raman tensors assume the form [3]

$$A = \begin{pmatrix} a & 0 \\ 0 & a \end{pmatrix} \quad E^T = \begin{pmatrix} c & 0 \\ 0 & -c \end{pmatrix} \quad E^L = \begin{pmatrix} 0 & -c \\ -c & 0 \end{pmatrix}. \quad (2)$$

Following the notation in [4], the susceptibility tensor can be expressed as:

$$\chi_{ijkl}^{(3)} = A_{ij} A_{kl} + E_{ij}^T E_{kl}^T + E_{ij}^L E_{kl}^L, \quad (3)$$

where each index can assume the values 1, 2 associated to the direction x and y respectively. Thus, the susceptibility tensor $\chi_{ijkl}^{(3)}$ gives rise to a 4×4 block-matrix

$$\begin{pmatrix} \begin{pmatrix} a^2 + c^2 & 0 \\ 0 & a^2 - c^2 \end{pmatrix} & \begin{pmatrix} 0 & c^2 \\ c^2 & 0 \end{pmatrix} \\ \begin{pmatrix} 0 & c^2 \\ c^2 & 0 \end{pmatrix} & \begin{pmatrix} a^2 - c^2 & 0 \\ 0 & a^2 + c^2 \end{pmatrix} \end{pmatrix}. \quad (4)$$

The first two indexes indicate the outer matrix elements and describe the polarization components of the emitted field (i index) and of the probe field (j index), while the last two indexes (k and l) indicate the inner matrix

elements and describe the polarization components of the two pump fields.

In particular, we are interested in selecting the excitation of an E symmetry Raman mode. For this purpose we use a probe linearly polarized along x and we perform a polarization selection after the sample in order to detect the emitted field component orthogonal to the probe (along y). This polarization configuration allows the selection of the susceptibility matrix elements $\chi_{21kl}^{(3)}$ associated with the involved E phononic mode. Notice that such elements vanish when $k = l$ that is when the two pump fields are both polarized along x or along y . Thus, in order to activate the process, we need the two pump fields (two frequency components of the same laser pulse) to have orthogonal polarizations. This is possible when the pump pulse is linearly polarized along a direction in between x and y . In particular, the efficiency of the ISRS is maximal when the pump polarization is at 45° with respect to the x axis. This is indeed the configuration we chose and consequently the matrix elements involved in our experiment are $\chi_{21kl(k \neq j)}^{(3)} = c^2$, getting an emitted field almost collinear with the unscattered probe photons and with polarization orthogonal to the probe one. We configure a polarizer after the sample in order to transmit the emitted field polarization only. The global polarization configuration is sketched in Fig 1. Note that a full extinction of the unscattered probe is experimentally not achievable (polarizer extinction rate 10^5). The residual probe acts as a local oscillator amplifying the emitted field within the total signal [5].

An effective fully quantum mechanical model for ISRS

The effective fully quantum mechanical approach to ISRS followed in the main text consists in the pump process, the subsequent dissipative, irreversible phonon dynamics and the probe process, all of them being described by quantum dynamical maps [6].

Before being hit by the pump laser beam described by photons in a multi-mode coherent state $|\bar{\nu}\rangle\langle\bar{\nu}|$, the relevant phonon mode at frequency Ω can be appropriately described by a thermal state at inverse temperature β

$$\rho_\beta = (1 - e^{-\beta\Omega}) e^{-\beta\Omega\hat{b}^\dagger\hat{b}}. \quad (5)$$

The pump process is described by a photon-phonon interaction Hamiltonian of the form

$$\mathcal{H} = \sum_{j,j'=-M}^M [g_{j,j'}^1 \mu_d (\hat{a}_{xj}^\dagger \hat{a}_{yj'} \hat{b}^\dagger + \hat{a}_{xj} \hat{a}_{yj'}^\dagger \hat{b}) + g_{j,j'}^2 \mu_s (\hat{a}_{xj}^\dagger \hat{a}_{yj'} (\hat{b}^\dagger)^2 + \hat{a}_{xj} \hat{a}_{yj'}^\dagger \hat{b}^2)], \quad (6)$$

where μ_d and μ_s are complex coupling constants and the functions $g_{j,j'}^\ell$ take into account the relations between the frequencies of the involved fields,

$$g_{j,j'}^\ell = \begin{cases} 1 & \text{if } j' = j + \frac{\ell\Omega}{\delta} \\ 0 & \text{elsewhere,} \end{cases} \quad \ell = 1, 2.$$

As stated in the main text, it should be noted that while the linear term involves only the creation of a phonon in a single mode at momentum $K = 0$, the quartic term are not limited to $K = 0$ and one should integrate over the entire optical phonon dispersion including processes where the momentum conservation is guaranteed by the creation of optical phonons with opposite momenta [7, 8]. In our effective Hamiltonian we include only a single phonon mode at $K = 0$. This assumption is made in view of the fact that in the experiments the probing process is limited to the linear regime and the phonons at different K will not affect the observed photon number fluctuations in this configuration.

The Hamiltonian in (6) generates an impulsive change of the initial photon-phonon state $|\bar{\nu}\rangle\langle\bar{\nu}| \otimes \rho_\beta$ given by

$$\rho^{\bar{\nu}} = \mathcal{U} (|\bar{\nu}\rangle\langle\bar{\nu}| \otimes \rho_\beta) \mathcal{U}^\dagger = |\bar{\nu}\rangle\langle\bar{\nu}| \otimes \mathcal{U}_{\bar{\nu}} \rho_\beta \mathcal{U}_{\bar{\nu}}^\dagger, \quad (7)$$

where, because of the high intensity of the pump laser beam, we have adopted the mean field approximation and substituted the photon annihilation and creation operators by the scalar amplitudes ν and ν^* and replaced \mathcal{U} with

$$\mathcal{U}_{\bar{\nu}} = \exp\{-i[c_1 \hat{b}^\dagger + c_1^* \hat{b} + c_2 (\hat{b}^\dagger)^2 + c_2^* \hat{b}^2]\} \quad (8)$$

$$c_1 = \mu_d \sum_{j,j'=-M}^M g_{j,j'}^1 \nu_{xj}^* \nu_{yj'} \quad (9)$$

$$c_2 = \mu_s \sum_{j,j'=-M}^M g_{j,j'}^2 \nu_{xj}^* \nu_{yj'} \quad (10)$$

The pump thus prepares the relevant phonon degree of freedom in a state $\rho_{II}^{\bar{\nu}}$ which is obtained from $\rho^{\bar{\nu}}$ by tracing over the photon degrees of freedom:

$$\rho_{II} = Tr_I \rho^{\bar{\nu}} = \mathcal{U}_{\bar{\nu}} \rho_\beta \mathcal{U}_{\bar{\nu}}^\dagger, \quad (11)$$

where II and I refer to the phonon and photon system, respectively.

The linear contribution in the phonon operators is responsible for the displacement of \hat{b} and \hat{b}^\dagger , while the quadratic one accounts for their multiplication by hyperbolic functions and thus for the possible squeezing of the corresponding quadratures [9, 11]:

$$\mathcal{U}_\nu^\dagger \begin{pmatrix} \hat{b} \\ \hat{b}^\dagger \end{pmatrix} \mathcal{U}_\nu = S \begin{pmatrix} \hat{b} \\ \hat{b}^\dagger \end{pmatrix} + \frac{1}{2|\beta|^2} (S-1) \begin{pmatrix} c_1 c_2^* \\ c_1^* c_2 \end{pmatrix} \quad (12)$$

$$S = \begin{pmatrix} \cosh(2|c_2|) & -e^{i(\phi-\frac{\pi}{2})} \sinh(2|c_2|) \\ -e^{-i(\phi-\frac{\pi}{2})} \sinh(2|c_2|) & \cosh(2|c_2|) \end{pmatrix}. \quad (13)$$

where $c_2 = |c_2|e^{i\phi}$. In order to write the squeezing matrix S in the standard formalism [9] we can define for convenience a complex squeezing parameter $\xi = re^{i\psi}$ with $r = 2|c_2|$ and $\psi = (\phi - \frac{\pi}{2})$.

The variance of the quadrature operator $\hat{B} = \frac{(\hat{b} + \hat{b}^\dagger)}{\sqrt{2}}$ with respect to the state ρ_{II}^ν is given by

$$\Delta_{\rho_{II}^\nu}^2 \hat{B} = Tr_{II} \left(\rho_{II}^\nu \hat{B}^2 \right) - \left(Tr_{II} \left(\rho_{II}^\nu \hat{B} \right) \right)^2 = \frac{1}{2} \coth \frac{\beta \Omega}{2} [\cosh(2r) + \sinh(2r) \cos \psi]. \quad (14)$$

Then, for $\psi = 0$ and r large enough, one can make $\Delta_{\rho_{II}^\nu}^2 \hat{B}$ smaller than $1/2$ which is the shot noise variance of \hat{B} with respect to the vacuum state $|0\rangle$ such that $\hat{b}|0\rangle = 0$.

The photoexcited phonon state ρ_{II}^ν then undergoes a dissipative dynamics that effectively takes into account the interaction of the phonons with their environment until, after a delay time τ , the target is hit by the probe laser beam. The phonon dynamics is considered to be that of an open quantum system in weak interaction with a large heat bath that will eventually drive the time-evolving phonon density matrix $\rho_{II}^\nu(t) = \rho_b(t)$ to a thermal state $\rho_{\beta'}$ at temperature T' larger than that of the pre-pump phonon state: $\beta' \leq \beta$. Such a relaxation process is described by a master equation [10] for the phonon density matrix $\rho_b(t)$ of the form $\partial_t \rho_b(t) = \mathbb{L}[\rho_b(t)]$, where the generator of the time-evolution is given by

$$\begin{aligned} \mathbb{L}[\rho_b(t)] &= -i \left[\Omega \hat{b}^\dagger \hat{b}, \rho_b(t) \right] \\ &+ \lambda (1 + n') \left(\hat{b} \rho_b(t) \hat{b}^\dagger - \frac{1}{2} \left\{ \hat{b}^\dagger \hat{b}, \rho_b(t) \right\} \right) \\ &+ \lambda n' \left(\hat{b}^\dagger \rho_b(t) \hat{b} - \frac{1}{2} \left\{ \hat{b} \hat{b}^\dagger, \rho_b(t) \right\} \right), \end{aligned} \quad (15)$$

where $n' = \frac{1}{e^{\beta' \Omega} - 1}$, while λ is a coupling constant sufficiently small so that the non-negligible presence of the environment can nonetheless be accounted for, in the so-called weak-coupling limit regime [10, 11], by a master equation of the above type.

The first term of \mathbb{L} generates the rotation in time of the phonon mode phase at its own eigenfrequency. The second two contributions consist of a so-called noise term $\hat{b} \rho_b(t) \hat{b}^\dagger$, respectively $\hat{b}^\dagger \rho_b(t) \hat{b}$ that has the property of transforming pure states into mixed states and of a dissipative term $-\frac{1}{2} \left\{ \hat{b}^\dagger \hat{b}, \rho_b(t) \right\}$, respectively $-\frac{1}{2} \left\{ \hat{b} \hat{b}^\dagger, \rho_b(t) \right\}$. These terms counterbalance the noise by keeping the trace of the time-evolving state $\rho_b(t)$, and thus the overall probability, constant in time. The anti-commutators can be incorporated into the Hamiltonian as anti-Hermitian contributions responsible for exponential time relaxation. The structure of \mathbb{L} is such that the generated time-evolution maps, formally $\gamma_t = \exp(t\mathbb{L})$, compose as a forward-in-time semigroup: $\gamma_t \circ \gamma_s = \gamma_s \circ \gamma_t = \gamma_{t+s}$ for all $s, t \geq 0$. Moreover, $\rho_b(t) = \gamma_t[\rho_b]$ can be explicitly computed for any initial phonon state ρ_b ; all initial states are eventually driven to a unique invariant state satisfying $\mathbb{L}[\rho_b] = 0$ that is given by the thermal state $\rho_{\beta'}$.

Finally, the probe process is again described by the Hamiltonian (6). However, the corresponding impulsive unitary operator $\mathcal{U} = \exp(-i\mathcal{H})$ now acts on a photon-phonon state of the form $|\bar{\alpha}\rangle \langle \bar{\alpha}| \otimes \rho_{II}^\nu(\tau)$. Here, $|\bar{\alpha}\rangle \langle \bar{\alpha}|$ is the multi-mode coherent state associated with the probe laser beam which contains x and y polarized components and is much smaller intense than the pump one, while $\rho_{II}^\nu(\tau)$ is the phonon state dissipatively evolved up to the delay time τ between pump and probe. Differently from the pump process, the lower probe intensity allows one to neglect in \mathcal{H} the terms responsible for the squeezing effects. Moreover, we can apply the mean field approximation only to the field operators with x polarization, since the x -polarized probe components are much more intense than those polarized along y . Then, by replacing \hat{a}_{xj} and \hat{a}_{xj}^\dagger by α_{xj} and α_{xj}^* the probe process is described by

$$\mathcal{U}_{\bar{\alpha}'} = \exp\{-i\|\bar{\alpha}'\|(\hat{A}(\bar{\alpha}') \hat{b}^\dagger + \hat{A}^\dagger(\bar{\alpha}') \hat{b})\}, \quad (16)$$

where $\hat{A}(\bar{\alpha}')$ is the collective photon annihilation operator

$$\hat{A}(\bar{\alpha}') = \frac{1}{\|\bar{\alpha}'\|} \sum_{j=-M}^M (\alpha_j')^* \hat{a}_{yj}, \quad \alpha_j' = \mu_d \sum_{j'=-M}^M g_{j',j}^1 \alpha_{xj}. \quad (17)$$

We can thus consistently let the probe process affect an initial state $|\bar{\alpha}_y\rangle\langle\bar{\alpha}_y| \otimes \rho_{II}^{\bar{\nu}}(\tau)$, where $|\bar{\alpha}_y\rangle = |\alpha_{y-M}\rangle \otimes \dots \otimes |\alpha_{y,M}\rangle$ is the coherent state involving only the y polarization components such that $\hat{a}_{yj}|\bar{\alpha}_y\rangle = \alpha_{yj}|\bar{\alpha}_y\rangle$. Notice that, unlike in (7), $\mathcal{U}_{\bar{\alpha}'}$ acts on the photon-phonon state as a whole and transforms it into

$$\mathcal{U}_{\bar{\alpha}'}|\bar{\alpha}_y\rangle\langle\bar{\alpha}_y| \otimes \rho_{II}^{\nu}(\tau)\mathcal{U}_{\bar{\alpha}'}^{\dagger}. \quad (18)$$

This allows for the quantum features of the phonon state and of its dynamics to be transcribed onto the emitted photon state

$$\rho_I(\tau) = \text{Tr}_{II} \left[\mathcal{U}_{\bar{\alpha}'}|\bar{\alpha}_y\rangle\langle\bar{\alpha}_y| \otimes \rho_{II}^{\nu}(\tau)\mathcal{U}_{\bar{\alpha}'}^{\dagger} \right]. \quad (19)$$

Unlike in the semi-classical theoretical approaches to pump and probe experiments attempted so far, one can here confront the experimental data with the scattered probe beam intensity, namely with the mean photon number $\langle\hat{N}_y\rangle_{\tau}$, where $\hat{N}_y = \hat{A}^{\dagger}(\bar{\alpha}')\hat{A}(\bar{\alpha}')$ and

$$\langle\hat{N}_y\rangle_{\tau} = \text{Tr} \left(\hat{N}_y \rho_I(\tau) \right), \quad (20)$$

and with its variance $\Delta_{\tau}^2 \hat{N}_y = \langle\hat{N}_y^2\rangle_{\tau} - \langle\hat{N}_y\rangle_{\tau}^2$.

Then one uses that

$$U_{\bar{\alpha}'}^{\dagger} \hat{N}_y U_{\bar{\alpha}'} = A^{\dagger}(\bar{\alpha}')\hat{A}(\bar{\alpha}') \cos^2(\|\bar{\alpha}'\|) + \hat{b}^{\dagger}\hat{b} \sin^2(\|\bar{\alpha}'\|) + \frac{i}{2} \sin(2\|\bar{\alpha}'\|)(A(\bar{\alpha}')\hat{b}^{\dagger} + A^{\dagger}(\bar{\alpha}')\hat{b}), \quad (21)$$

where, given the experimental conditions effectively described by the model, it is plausible to set all amplitudes $\alpha_{xj} = \alpha_x$ and $\alpha_{yj} = \alpha_y = |\alpha_y|\exp(i\theta_y)$, in which case

$$\alpha'_j = \mu_d \alpha_x = |\mu_d \alpha_x| e^{i\theta'}, \quad \text{and} \quad \|\bar{\alpha}'\| = \sqrt{K}|\mu_d \alpha_x|, \quad (22)$$

where $K = 2M + 1$ is the total number of modes within a mode-locked optical pulse.

By denoting with $I_y = K|\alpha_y|^2$ the pulse intensity for the y polarization and using that

$$\hat{a}(\bar{\alpha}')|\bar{\alpha}_y\rangle = \sqrt{I_y}e^{-i(\theta' - \theta_y)}|\bar{\alpha}_y\rangle, \quad (23)$$

one can thus explicitly compute:

$$\langle\hat{N}_y\rangle_{\tau} = I_y \cos^2(\|\bar{\alpha}'\|) + \sin^2(\|\bar{\alpha}'\|) \langle\hat{b}^{\dagger}\hat{b}\rangle_{\tau} + \frac{i}{2} \sqrt{I_y} \sin(2\|\bar{\alpha}'\|) (e^{-i(\theta' - \theta_y)} \langle\hat{b}^{\dagger}\rangle_{\tau} - e^{i(\theta' - \theta_y)} \langle\hat{b}\rangle_{\tau}), \quad (24)$$

where $\langle\hat{O}\rangle_{\tau} = \text{Tr}_{II} \left(\rho_{II}^{\bar{\nu}}(\tau) \hat{O} \right)$ is the expectation value of any phonon operator \hat{O} with respect to the phonon state $\rho_{II}^{\bar{\nu}}(\tau)$.

Despite its complicated expression, we report also the number variance predicted by the model as $\langle\hat{N}_y\rangle_{\tau}$ and $\Delta_{\tau}^2 \hat{N}_y$ are the quantities computed numerically in the main text and compared with the experimental data:

$$\begin{aligned} \Delta_{\tau}^2 \hat{N}_y &= I_y \cos^4(\|\bar{\alpha}'\|) + \sin^4(\|\bar{\alpha}'\|) \left(\langle(\hat{b}^{\dagger}\hat{b})^2\rangle_{\tau} - \langle\hat{b}^{\dagger}\hat{b}\rangle_{\tau}^2 \right) + \sin^2(\|\bar{\alpha}'\|) \cos^2(\|\bar{\alpha}'\|) \langle\hat{b}^{\dagger}\hat{b}\rangle_{\tau} \\ &- I_y \sin^2(\|\bar{\alpha}'\|) \cos^2(\|\bar{\alpha}'\|) \left[e^{-2i(\theta' - \theta_y)} \left(\langle(\hat{b}^{\dagger})^2\rangle_{\tau} - \langle\hat{b}^{\dagger}\rangle_{\tau}^2 \right) + e^{2i(\theta' - \theta_y)} \left(\langle\hat{b}^2\rangle_{\tau} - \langle\hat{b}\rangle_{\tau}^2 \right) \right] \\ &+ I_y \sin^2(\|\bar{\alpha}'\|) \cos^2(\|\bar{\alpha}'\|) \left(2\langle\hat{b}^{\dagger}\hat{b}\rangle_{\tau} + 1 - 2\langle\hat{b}^{\dagger}\rangle_{\tau} \langle\hat{b}\rangle_{\tau} \right) \\ &+ i\sqrt{I_y} \sin(\|\bar{\alpha}'\|) \cos^3(\|\bar{\alpha}'\|) \left(e^{-i(\theta' - \theta_y)} \langle\hat{b}^{\dagger}\rangle_{\tau} - e^{i(\theta' - \theta_y)} \langle\hat{b}\rangle_{\tau} \right) \\ &+ i\sqrt{I_y} \sin^3(\|\bar{\alpha}'\|) \cos(\|\bar{\alpha}'\|) \left[2e^{-i(\theta' - \theta_y)} \left(\langle(\hat{b}^{\dagger})^2\hat{b}\rangle_{\tau} - \langle\hat{b}^{\dagger}\hat{b}\rangle_{\tau} \langle\hat{b}^{\dagger}\rangle_{\tau} + \frac{1}{2} \langle\hat{b}^{\dagger}\rangle_{\tau}^2 \right) \right. \\ &\left. - 2e^{i(\theta' - \theta_y)} \left(\langle\hat{b}^{\dagger}\hat{b}^2\rangle_{\tau} - \langle\hat{b}^{\dagger}\hat{b}\rangle_{\tau} \langle\hat{b}\rangle_{\tau} + \frac{1}{2} \langle\hat{b}\rangle_{\tau}^2 \right) \right] \end{aligned} \quad (25)$$

The phononic correlation functions involving \hat{b} and \hat{b}^{\dagger} contribute with oscillations at frequency Ω while those involving \hat{b}^2 and $\hat{b}^{\dagger 2}$ give rise to 2Ω oscillations; collecting the corresponding coefficients one finds the following amplitude for the 2Ω oscillating component in $\Delta_{\tau}^2 \hat{N}_y$:

$$A_{2\Omega} = \frac{I_y(1+2n')}{4} e^{-\lambda t} \sin^2(2\|\bar{\alpha}'\|) \sinh(2r), \quad (26)$$

where the squeezing parameter $r = 2|c_2| = 4K|\mu_s||\nu|^2$ is obtained from (10) by putting all pump amplitudes equal to ν . Moreover we take λ to comply with the observed oscillation time-scale and the time $t > 0$ such that $\lambda t \ll 1$.

In the last figure in the main text we have shown the $A_{2\Omega}$ predicted by the model together with the experimental results for different pump intensities. We found an optimal value of the coupling parameter c_2 for which the model agrees with the experiments. We used such a value for computing the squeezing parameter r for all the experimental pump fluences. In particular $|\nu|^2$ is the number of photons per unit cell per pulse. We then computed the uncertainties in the position and momentum phonon operator as in (14). The results reported in the main text unveil photo-excited thermal squeezed vibrational states.

Single pulse differential acquisition system in shot-noise limited regime

The acquisition system is made of a balanced amplified differential photodetector and a fast digitizer (*Spectrum M3i.2132-exp*) with sampling rate 1 GS/s. The differential photodetector consists of two *Hamamatsu S3883* Silicon PIN photodiodes with 0.94 quantum efficiency connected in reverse bias and followed by a low-noise charge amplifier. The photo-currents generated by the two photodiodes in response to a single optical pulse impinging on them are physically subtracted and the resulting charge is amplified using *CAEN* designed electronic components. In particular, the preamplifier sensitivity is 5.2 mV/fC with a linear response up to about 2 V of pulse peak. In order to distinguish the intrinsic noise (shot noise) from other contributions, we tested the experimental set-up in absence of the pump. The variance ΔT_{var} of 8000 differential pulses is measured for different powers of the probe. The optical noise, shown in Fig 2, is linear with a constant offset representing the electronic noise. This behavior is characteristic of the shot-noise regime [12]. We chose a probe power within the linearity interval (2.5 mW, 0.2 mJ/cm² on the sample). This provides a reference for the shot noise value of 1.1 V² which is used to benchmark the noise in time domain experiments and avoid additional noise sources.

The detector shot noise linearity test demonstrates that we are sensible to quantum fluctuations of the photon number. In particular, the shot-to-electronic noise at the maximum probe intensity in the linear regime is approximately 10 dB.

References

- [1] Etchepare, Grillon, Chambaret, Hamoniaux, and Orszag. Polarization selectivity in time-resolved transient phase grating. *Optic. Comm.*, 63, 1987.
- [2] Scott and Porto. Longitudinal and transverse optical lattice vibrations in quartz. *Physical Review*, 161, 1967.
- [3] P. Umari, Alfredo Pasquarello, and Andrea Dal Corso. Raman scattering intensities in α -quartz: A first-principles investigation. *Phys. Rev. B*, 63:094305, 2001.
- [4] Andy Rundquist, Jon Broman, David Underwood, and David Blank. Polarization-dependent detection of impulsive stimulated raman scattering in alpha-quartz. *Journal of Modern Optics*, 52, 2006.
- [5] Shaul Mukamel. *Principles of Nonlinear optical spectroscopy*. Oxford University Press, 1995.
- [6] Kelvin Titimbo. *Creation and detection of squeezed phonons in pump and probe experiments: a fully quantum treatment*. PhD thesis, University of Trieste, 2015.
- [7] B Dorner and H Grimm and H Rzany. *Phonon dispersion branches in a quartz*. *Journal of Physics C: Solid State Physics*, 13:6607, 1980.
- [8] J. F. Scott. *Evidence of Coupling Between One- and Two-Phonon Excitations in Quartz*. *Phys. Rev. Lett.*, 21:907–910, 1968.
- [9] M. O. Scully and M. S. Zubairy. *Quantum Optics*. Cambridge University Press, Cambridge UK, 1997.
- [10] R. Alicki and K. Lendi. *Quantum Dynamical Semigroups and Applications, Lect. Notes Phys.* 717. Springer-Verlag, Berlin, 2007.
- [11] H.-P. Breuer and F. Petruccione. *Quantum Optics*. Oxford University Press, New York UK, 2002.
- [12] H. A. Bachor and T. C. Ralph. *A Guide to Experiments in Quantum Optics*. New York: Wiley, 2004.

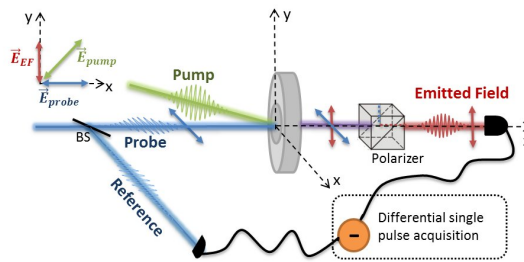


Figure 1: Scheme of the experimental setup.

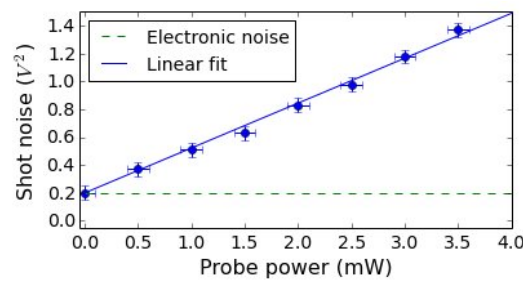


Figure 2: Characterization of the probe noise in absence of the pump: variance of 8000 acquired differential pulses as a function of the probe power.